THE BELL SYSTEM TECHNICAL JOURNAL
Vol. 59, No. 6, July–August 1980
*Printed in U.S.A.*

# Frequency-Hopping, Multiple-Access, Phase-Shift-Keying System Performance in a Rayleigh Fading Environment

By O. YUE

(Manuscript received October 31, 1979)

*Recently, various Frequency-Hopping, Multiple-Access (FHMA) schemes have been proposed as alternatives to frequency-division (FDMA) techniques for guarding against interference from other users and multipath fading in transmitting digitized speech in mobile radio. While the advantage of frequency diversity against fading is well known, the system degradation of frame-asynchronous FHMA-PSK due to interference from other users and fading has not been studied, except by modeling the interference as additive white Gaussian noise (AWGN). In this paper, we analyze the performance of two FHMA-PSK systems in a Rayleigh fading environment. We assume that the interferers' addresses are assigned at random and derive expressions for the union upper bound on the bit error rate ($P_b$) for U users, each assigned N frequencies, i.e., N chips. As an example, we consider transmitting digitized speech ($R$ = 31.25 kb/s) over the mobile radio channel (bandwidth $W$ = 20 MHz), using orthogonal coding of rate $r = 5/32$ ($N = 32$). For the differentially coherent FHMA-PSK case, the number of users in a two-way radio system is limited to 26 by the performance of the mobile-to-base link, which corresponds to an equivalent bandwidth of 770 kHz per user.*

## I. INTRODUCTION

Two major impairments of mobile radio communication systems are interference from other users and multipath fading. The frequency-division, multiple-access (FDMA) technique uses guard bands between frequency channels to minimize interference and increased signal power to combat fading. Recently, various frequency-hopping (FH) techniques have been proposed for transmitting digitized speech in mobile radio, including a differential phase-shift-keyed (DPSK) system[1] and a multilevel frequency-shift-keyed (MFSK) system.[2]

The FHMA approach uses frequency diversity against fading and keeps the interference down to an acceptable level by properly designing the set of frequency-hopping patterns (addresses) assigned to the users. While the effectiveness of diversity schemes in a fading environment with no interference is well known, the system degradation of the frame asynchronous FHMA-PSK scheme due to other user interference has not been analyzed, except by modeling the interference as additive white Gaussian noise (AWGN).[1]

In this paper, we study the performance of FHMA-PSK systems with orthogonal coding (Ref. 3, p. 232) in a Rayleigh fading environment using both coherent and differentially coherent detection. (Empirical evidence shows that the Rayleigh model is accurate for urban mobile radio situtations.[4]) The approach of using coding and soft-decision decoding on multiple access channels is similar to that studied in Ref. 5, although the modulation technique is different. However, in Ref. 5 and in recent extensions,[6,7] the fading model is not only frequency selective, but also fast fading, while the fading in our model is slow enough to allow coherent or differentially coherent detection. Instead of using the AWGN model[1] or the worst-case, partial-band interference model,[5] we assume that the interferers' addresses are assigned at random and derive expressions for the union upper bound of the bit error rate ($P_b$) for $U$ users, each assigned $N$ frequencies, i.e., $N$ chips.

In Section II, we define the transmitted signal set and the received waveforms for $K$ orthogonal frequency channels. An example of transmitting digitized speech is also described. The correlation receiver is analyzed in Section III. For the base-to-mobile transmission, frame synchronism among all users can be maintained so that there is no interference, and the full advantage of frequency diversity can be realized for $U = K$ users, which is the same number of users accommodated by FDMA-PSK. In the mobile-to-base case, we assume chip synchronization among users and show that, with $U = K$ users, the FHMA-PSK system degrades by 5 dB at $P_b = 10^{-3}$. We also determine the bit error rate versus the number of users in the limit of no receiver noise. The same analysis is repeated in Section IV for the differentially coherent receiver.

## II. TRANSMITTED AND RECEIVED SIGNALS

We define a set of orthogonal functions over the bandwidth $(f_0, f_0 + W)$ with $f_0 \gg W$ and time interval $[0, T)$ as:

$$\psi_{kn}(t) = \begin{cases} \sqrt{2S}\sin(\Omega_k t), & t \epsilon \tau_n = [(n-1)t_1, nt_1) \\ 0, & \text{otherwise} \end{cases} \tag{1}$$

for $k = 1, 2, \cdots, K$ and $n = 1, 2, \cdots, N$, with $\Omega_k = 2\pi(f_0 + kf_1)$, $f_1 = W/K$, $t_1 = T/N$ and

$$f_1 t_1 = 1. \tag{2}$$

(Section V, Conclusions, has a discussion on the $f_1 t_1 < 1$ case.[1]) The energy of each function is $St_1$, and $KN = WT$ elements are in this set. (We could obtain $WT$ additional orthogonal functions by changing "sin" to "cos" in (1), but they will not be used in this paper.) We shall refer to intervals of $T$ and $t_1$ as frames and chips, respectively.

### 2.1 Frequency-hopping, phase-shift-keyed signals

A user is assigned a $K$-by-$N$ address matrix $\mathbf{A}$ with $N$ unity elements, one in each column, and $N(K-1)$ zeros. For frequency diversity, it is desirable to have not more than one nonzero element in each row of $\mathbf{A}$. Then the FH carrier of this user during one frame is given by

$$c(t) = \sum_{n=1}^{N} \sum_{k=1}^{K} \mathbf{A}(k, n)\psi_{kn}(t) = \sum_{n=1}^{N} x_n(t), \tag{3}$$

where

$$x_n(t) = \begin{cases} \sqrt{2S} \sin \omega_n t, & t \epsilon \tau_n \\ 0 & \text{otherwise} \end{cases}$$

with $\omega_n = \Omega_{k_n}$ and $k_n$ defined by $\mathbf{A}(k_n, n) = 1$. The user's data is first coded using an $N$-by-$N$ Hadamard matrix (Ref. 3, p. 232) with elements $h_{nm} = \pm 1$. The block encoder accepts $\log_2 N$ bits of information and outputs an $N$ bit word, so its code rate is $r = \log_2 N/N$. Since the vectors $\{\bar{h}_m\}$ of a Hadamard matrix $\mathbf{H}$ agree pairwise in as many elements as they disagree, they are mutually orthogonal. Then, using biphase modulation, we obtain $N$ orthogonal waveforms for transmission:

$$s_m(t) = \sum_{n=1}^{N} h_{nm} x_n(t), \qquad m = 1, 2, \cdots, N. \tag{4}$$

The energy of each waveform is $ST \triangleq E$, and the transmission rate ($R$) is $(\log_2 N)/T$ b/s.

### 2.2 Effects of fading and interference

We assume that the frequency spacing $f_1$ is large enough so that the medium between the transmitter and the receiver can be modeled as $N$ independent Rayleigh fading channels. Then, upon reception, the $m$th transmitted signal, corresponding to the code word $\bar{h}_m$, becomes

$$\hat{s}_m(t) = \sum_{n=1}^{N} h_{nm} \alpha_n x_n(t + \phi_n/\omega_n), \qquad 0 \le t < T, \tag{5}$$

where the $\alpha_n$'s have the same probability density function:

$$p(\alpha_n) = 2\alpha_n \exp(-\alpha_n^2), \qquad 0 \le \alpha_n < \infty,$$

and the phase angle $\phi_n$ is uniformly distributed between 0 and $2\pi$.

Let the total number of simultaneous users be $U = J + 1$. Then the interference due to the $J$ other users (interferers) can be written as:

$$I(t) = \sum_{j=1}^{J} \gamma_j \sum_{n=1}^{N} b_{nj} \sum_{k=1}^{K} \mathbf{B}_j(k, n)\beta_{kj}\psi_{kn}(t + \theta_{kj}/\Omega_k), \qquad 0 \le t \le T, \tag{6}$$

where

| | |
|---|---|
| $\mathbf{B}_j$ | is the address matrix of the $j$th interferer (with the columns shifted if the users are not frame-synchronized), |
| $b_{nj}$ | $= \pm 1$ is modulation of the $j$th interferer in the interval $\tau_n$, |
| $\gamma_j^2 S$ | is the unfaded power of the $j$th interferer, |
| $\beta_{kj}$ | is Rayleigh distributed with unit variance, |
| $\theta_{kj}$ | is uniformly distributed between 0 and $2\pi$, |

and all the above random variables are independent of one another and also the $\alpha_n$'s and $\phi_n$'s in (5).

Finally, the received signal is given by

$$r(t) = \hat{s}_m(t) + I(t) + n(t), \qquad 0 \le t \le T,$$

where $n(t)$ is stationary white Gaussian noise, with one-sided power spectral density $N_0$.

### 2.3 An example

To illustrate the performance of the FHMA-PSK systems, we consider the case of transmitting digitized speech ($R$ = 31.25 kb/s) over a bandwidth $W$ = 20 MHz using a Hadamard code of rate $r = 5/32$, i.e., $N = 32$. The bandwidth is divided into $K = rW/R = 100$ channels, with frequency spacing $f_1 = 200$ kHz; the frame $T$ and chip $t_1$ intervals are 0.16 ms and 5 $\mu$s, respectively. FDMA systems, using the same coding and modulation schemes, can accommodate 100 users with no interference and the performance is limited only by fading. A typical requirement for acceptable quality of digitized speech is an error rate ($P_b$) of $10^{-3}$ and, if there is no power limitation, FDMA can always meet the performance requirement by increasing transmitted power.

## III. CORRELATION RECEIVER

For a set of known, constant $\alpha_n$'s, the optimum detector for $N$ equally likely waveforms with no interference consists of $N$ correlators.

The $l$th correlator output at $t = T$ is

$$Z_l = \int_0^T r(u)\hat{s}_l(u)\,du$$

$$= \sum_{n=1}^{N} h_{nl} \int_{\tau_n} r(u)\alpha_n\sqrt{2S}\sin(\omega_n u + \phi_n)\,du \triangleq \sum_{n=1}^{N} h_{nl}Y_n. \qquad (7)$$

An implementation of the correlation receiver is shown in Fig. 1. The decision rule is to choose the code word $\bar{h}_l$ corresponding to the largest $Z_l$ as being the one transmitted.

### 3.1 Statistical properties of the correlator outputs

The component of the interference due to the $j$th interferer affecting the $n$th correlator output is given by

$$I_{nj}(t) = \gamma_j b_{nj}\mathbf{B}_j(k_n, n)\beta_{k_n j}\sqrt{2S}\sin(\omega_n t + \theta_{k_n j})$$

$$= \xi_{nj}\sqrt{2S}\sin(\omega_n t + \phi_n) + \eta_{nj}\sqrt{2S}\cos(\omega_n t + \phi_n),\ t\epsilon\tau_n, \qquad (8)$$

where $\xi_{nj}$ and $\eta_{nj}$ are independent, identically distributed (i.i.d.) Gaus-

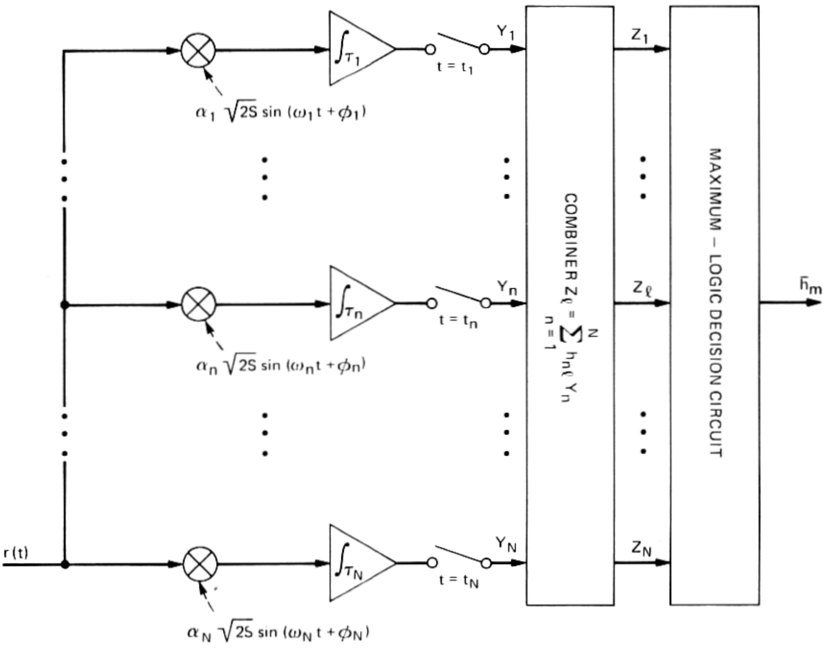


Fig. 1—Correlation receiver for FHMA-PSK signals. The coefficients in the linear combiner are elements of a Hadamard matrix. The decision circuit chooses the code word $\bar{h}_m$, corresponding to the largest $Z_m$.

sian random variables with zero mean and variance $\lambda_{nj}/2$, with $\lambda_{nj} \triangleq \gamma_j^2 \mathbf{B}_j(k_n, n)$. We note that the Gaussianity of $I_{nj}(t)$ is conditional on the random variable $\mathbf{B}_j(k_n, n)$; $\gamma_j$ is assumed to be deterministic, which means we ignore the effect of "shadow" fading on path loss.

If the transmitted waveform is $s_m(t)$, then the $n$th integrator output is given by

$$Y_n = \alpha_n E_c(\alpha_n h_{nm} + \sum_{j=1}^{J} \xi_{nj} + G_0), \tag{9}$$

where the energy per chip is

$$E_c = E/N,$$

and $G_0$ is Gaussian with zero mean and variance

$$d/2 = N_0/2E_c.$$

Therefore, conditioned on $\alpha_n$ and the $\lambda_{nj}$'s, the characteristic function of $Y_n$ is given by

$$E[e^{iuY_n} \,|\, \alpha_n, \Gamma_n] = \exp \alpha_n^2 \left[ iuh_{nm} E_c - \frac{u^2 E_c^2}{4} (\Gamma_n + d) \right],$$

where $\Gamma_n = \sum_{j=1}^{J} \lambda_{nj}$ is the sum of $J$ independent random variables. Averaging over $\alpha_n$, we obtain

$$E[e^{iuY_n} \,|\, \Gamma_n] = \left[ 1 - iuE_c h_{nm} + \frac{u^2 E_c^2}{4} (\Gamma_n + d) \right]^{-1}. \tag{10}$$

In general, the statistics of $\Gamma_n$ depend on the set of user addresses and the degree of synchronization among the users; two specific cases are analyzed in later sections. However, we shall assume that the $\Gamma_n$'s are identically distributed and independent from chip to chip.

### 3.2 Error probability

The probability of a word error for the correlation receiver is given by

$$P_e = \frac{1}{N} \sum_{m=1}^{N} \Pr \left[ \bigcup_{\substack{l=1 \\ l \neq m}}^{N} (Z_m \leq Z_l) \,|\, m\text{th signal transmitted} \right],$$

which is bounded by

$$\frac{1}{N} \sum_{m=1}^{N} \operatorname*{Max}_{l \neq m} \Pr[Z_m - Z_l \leq 0 \,|\, m] \leq P_e \leq \frac{1}{N} \sum_{m=1}^{N} \sum_{\substack{l=1 \\ l \neq m}}^{N} \Pr[Z_m - Z_l \leq 0 \,|\, m].$$

From (7), we have

$$Z_m - Z_l = \sum_{n=1}^{N} (h_{nm} - h_{nl}) Y_n = \sum_{i=1}^{L} 2h_{n_i m} Y_{n_i} \tag{11}$$

where $n_i$ is defined by $h_{n_i m} = -h_{n_i l}$, and from the definition of $\mathbf{H}$ there are exactly $L = N/2$ $n_i$'s. From (10) and the mutual independence of the $\Gamma_n$'s, we can see that each of the summands in (11) are independent and identically distributed, so that the error probability of a pairwise comparison is given by the inverse Fourier integral (Ref. 14, p. 271):

$$\Pr[Z_m - Z_l \leq 0 \,|\, m] = -\frac{1}{2\pi i}\int_c \Phi^L(z)\, dz/z \triangleq P_p, \tag{12}$$

where

$$\Phi(z) = E_\Gamma[\{1 - 2iz + z^2(\Gamma + d)\}^{-1}], \tag{13}$$

with $E_\Gamma[\ ]$ denoting expectation with respect to the random variable $\Gamma$, and with the path of integration $c$ along the real axis except for an indentation above the origin.

We observe that $\Pr[Z_m - Z_l \leq 0 \,|\, m]$ is the same for all $l \neq m$, so the bounds in $P_e$ become

$$P_p \leq P_e \leq (N - 1)P_p.$$

Since $\log_2 N$ bits of information are conveyed by each transmitted waveform, the bit error rate is related to $P_e$ by $P_b = NP_e/(2(N - 1))$ (Ref. 3, p. 240), and is bounded by

$$\frac{N}{2(N-1)} P_p \leq P_b \leq \frac{N}{2} P_p. \tag{14}$$

### *3.3 Frame synchronous case—no interference*

When the base station transmits to the mobiles, it is reasonable to require frame synchronization among all users so that the $\mathbf{B}_j(k, n)$ in (6) is the unshifted address of the $j$th user. Moreover, for $K$ frequency channels, there are $K$ orthogonal addresses, which means that for $J < K$ the transmission from base to mobile is interference-free and the system performance is limited only by fading and noise.

In terms of the random variable $\lambda_j$ (the dependence on $n$ has been removed), the interference-free case is characterized by the probability density function

$$p(\lambda_j) = \delta(\lambda_j).$$

Then $\Phi(z)$ in (13) becomes

$$\Phi(z) = [1 - 2iz + z^2 d]^{-1},$$

which means the integrand in (12) has an $L$th-order pole at $z_0 = i(1 + \sqrt{(1 + d)})/d$. The error probability of pairwise comparisons can be evaluated by computing the residue at $z_0$:

$$P_p = 2^{-L}\left(1 - \sqrt{\frac{1}{1+d}}\right)^L \sum_{k=0}^{L-1} \binom{L-1+k}{k} 2^{-k}\left(1 + \sqrt{\frac{1}{1+d}}\right)^k, \tag{15}$$

which has also been derived by Bello and Nelin [Ref. 8, eq. (37)].

Substituting (15) into (14), we plot the upper bound on the bit error rate in Fig. 2 for the example described in Section 2.3, i.e., $N = 32$, $K = 100$. The abscissa is $E_b/N_0$, where $E_b = E/\log_2 N$ is the energy per bit. To illustrate the advantage of frequency diversity, we also plot the performance of FDMA-PSK, with

$$P_p = \frac{1}{2}\left[1 - \sqrt{\frac{1}{1+d_1}}\right], \tag{16}$$

which is the $L = 1$ case of (15) with $d_1^{-1} = E/2N_0$, the average SNR with fading. Observe that, at $P_b \cong 10^{-3}$, FHMA requires 26 dB less power than FDMA.

### 3.4 Frame asynchronous (chip synchronized) case

In the mobile-to-base transmission, we assume that all the users are chip-synchronized. In addition, a power control strategy is assumed to be implemented so that the unfaded power from all users as received by the base station is the same ($\gamma_j = 1$).

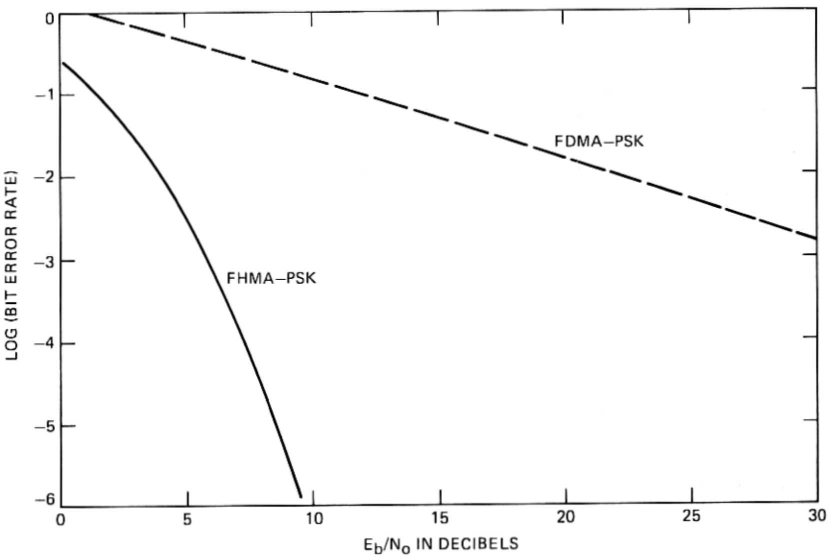


Fig. 2—Comparison between frame-synchronous FHMA and FDMA using coherent PSK and Hadamard coding with rate 5/32 for 100 users sharing 100 frequency channels ($E_b/N_0$ = energy per bit/receiver noise spectral density).

### 3.4.1 Random addressing*

We shall assume that the probability of an interferer transmitting $\omega_n$ in $\tau_n$ is $\mu = 1/K$; this assumption can be justified either from a random addressing argument or from the asynchronism among the users. Then the probability density function of $\lambda_j$ is given by

$$p(\lambda_j) = (1 - \mu)\delta(\lambda_j) + \mu\delta(\lambda_j - 1), \tag{17}$$

and $\Gamma$ is binomially distributed:

$$\Pr[\Gamma = k] = B(k, J) \triangleq \frac{J!}{k!(J-k)!}\mu^k(1-\mu)^{J-k}, \qquad k = 0, 1, 2, \cdots, J.$$

Performing the expectation in (13), we obtain

$$\Phi(z) = \sum_{k=0}^{J} B(k, J)/[1 - 2iz + z^2(k + d)], \tag{18}$$

which has $J + 1$ poles in the upper half plane:

$$z_k = i(1 + \sqrt{1 + k + d})/(k + d).$$

As in the frame-synchronized case, $P_p$ can be computed by evaluating the residues at the $z_k$'s, but for large $J$ and large $L$, the procedure is very tedious. Fortunately, the saddle-point method[9] is well suited for computing integrals like (12) for $L \gg 1$.

Define $G(z) = \ln\Phi(z)$ and $z_s = iy_s$ to be a saddle point on the imaginary axis as given by

$$G'(z_s) = 0. \tag{19}$$

Then deforming the path of integration in (12) to pass through $z_s$ and substituting the Taylor series expansion around $z_s$ for $G(z)$:

$$\begin{aligned} G(z) &= G(z_s) + \frac{1}{2}(z - z_s)^2 G''(z_s) + \cdots \\ &= G_s - \frac{1}{2}(z - iy_s)^2\sigma_s^2 + \cdots, \end{aligned} \tag{20}$$

we can integrate term-by-term to obtain an asymptotic series in $L$. The leading term is given by

$$P_p \sim \frac{1}{2}\exp\left[LG_s + \frac{L}{2}\sigma_s^2 y_s^2\right]\operatorname{erfc}\left[\sqrt{\frac{L}{2}}\,\sigma_s y_s\right]. \tag{21}$$

A discussion on the computation of (21) is given in the appendix.

* Similar to the random coding arguments (Ref. 14, p. 25), the error probability obtained in this section provides an upper bound to that achieved with an optimum assignment of addresses.

Substituting (21) into (14), we plot $P_b$ for the same example in Section 2.3 versus $E_b/N_0$ for $U = 100$ users in Fig. 3. At $P_b = 10^{-3}$, the system performance degrades by about 5 dB due to interference. However, for the same number of users, FHMA-PSK still requires 21 dB less in power than FDMA-PSK.

In Fig. 3, we can see that, for $E_b/N_0$ larger than 15 dB, $P_b$ begins to level off and the system performance becomes interference-limited. For the noise-free case ($d = 0$), where degradation is due only to interference, we plot $P_b$ as a function of the number of users $U$ in Fig. 4.

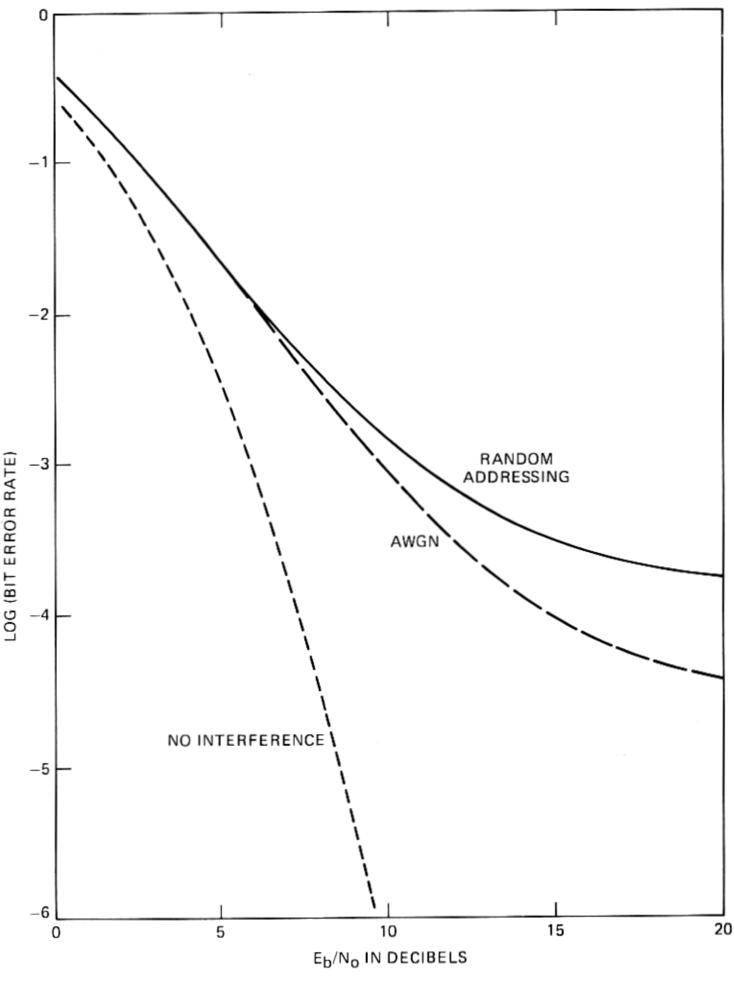


Fig. 3—Performance of frame-asynchronous FHMA-PSK for 100 users. The AWGN result is obtained by modeling the interference as additive white Gaussian noise.

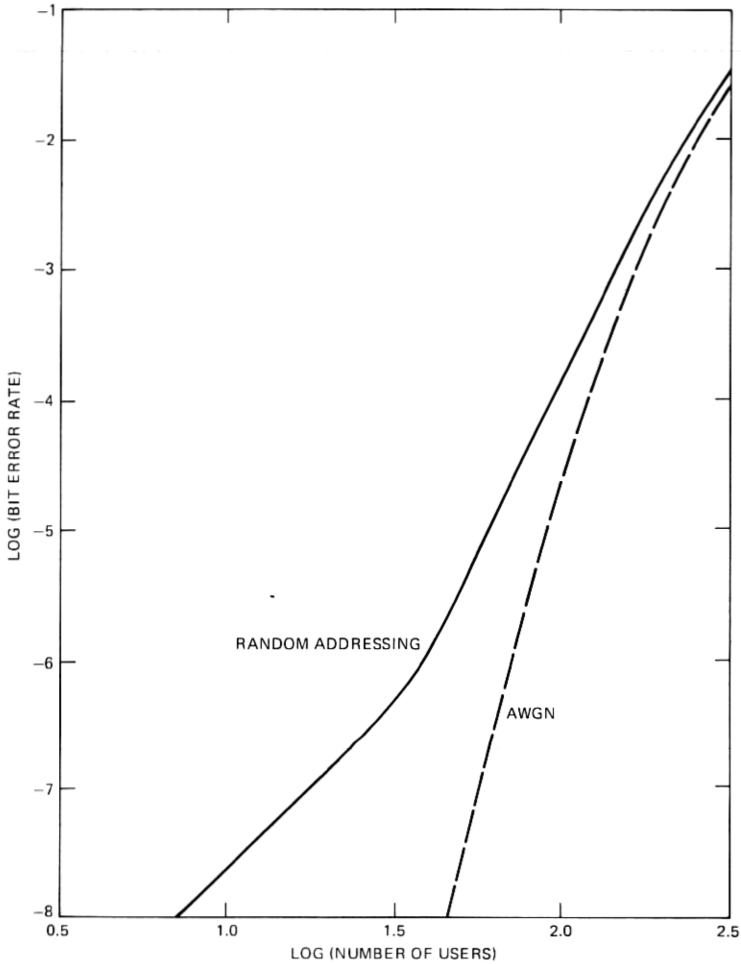


Fig. 4—Interference-limited performance of frame-asynchronous FHMA-PSK (no receiver noise). There are 100 frequency channels available.

### 3.4.2 *Modeling interference as AWGN*

Previous analysis[1] has treated the net effect of interference as an increase in receiver noise which is assumed to be additive, white Gaussian noise (AWGN). Then the contribution of such interference would be *unconditionally* Gaussian with normalized variance $(S/W)/E_c = 1/K$; this is equivalent to approximating (17) with

$$p(\lambda_j) = \delta(\lambda_j - \mu). \tag{22}$$

Using the above in (13), we obtain $P_p$ as given by (15), but with $d = N_0/E_c + (U - 1)/K$.

The result under the AWGN assumption for $U = 100$ users is included in Fig. 3. At $P_b = 10^{-3}$, this model underestimates the required SNR by about 1 dB. The interference limited case is plotted in Fig. 4. For small $P_b(\sim 10^{-6})$, the AWGN approximation overestimates the maximum number of users by a factor of 2, but for $P_b = 10^{-3}$, the deviation is only about 15 percent.

## IV. DIFFERENTIALLY COHERENT RECEIVER

When the amplitude ($\alpha_n$) and phase ($\phi_n$) of the desired signal are not known at the receiver, coherent detection is not possible. In this section, we analyze the differential PSK (DPSK) system[12] which requires amplitude and phase coherence over an interval of $T$ s. The transmitted data are precoded so that the information is conveyed by the phase change from frame to frame. The decoding is accomplished by "phase comparators" which replace the multiplier-integrator combinations in the coherent receiver. The structure of the differential receiver is shown in Fig. 5.

### *4.1 Statistical properties of the phase comparator outputs*

The $n$th phase comparator consists of a bandpass filter of gain $\sqrt{t_1}$

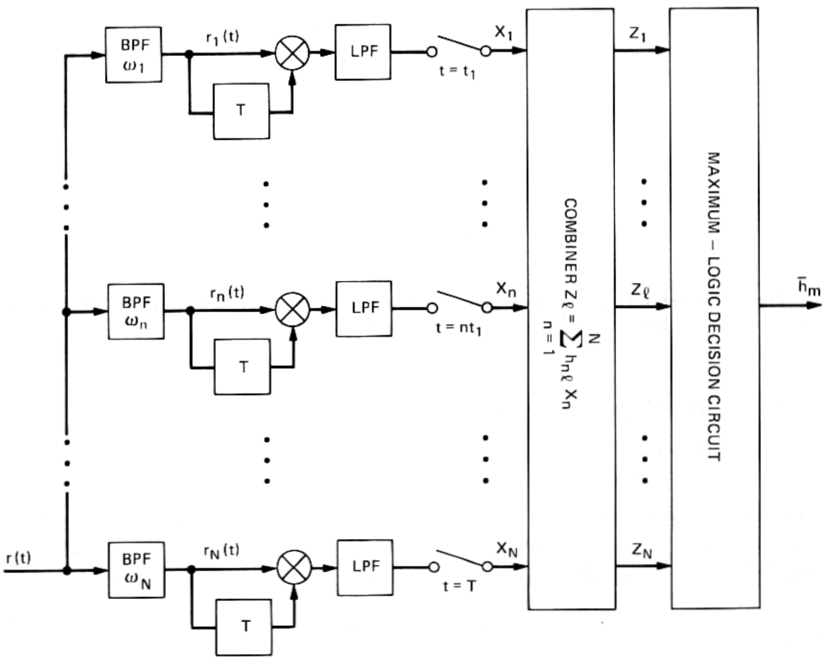


Fig. 5—Differentially coherent receiver for FHMA-DPSK signals. The bandpass filter (BPF) in the $n$th branch has gain $\sqrt{t_1}$ and bandwidth $1/t_1$ centered at $\omega_n$.

and bandwidth $1/t_1$ centered at $\omega_n$, a time delay $T$, a multiplier, and a lowpass filter. If the transmitted waveform is $\tilde{s}_q(t)$, then the output of this bandpass filter in interval $\tau_n$ is given by

$$r_n(t) = \left[\alpha_n \tilde{h}_{nq} + \sum_{j=1}^{J} \xi_{nj} + \xi_0(t)\right] \sqrt{2E_c}\sin(\omega_n t + \phi_n) + \left[\sum_{j=1}^{J} \eta_{nj} + \eta_0(t)\right] \sqrt{2E_c}\cos(\omega_n t + \phi_n), \quad (23)$$

where $\xi_{nj}$ and $\eta_{nj}$ are as defined in Section 3.1 and $\xi_0(t)$ and $\eta_0(t)$ are zero-mean, Gaussian processes with $\mathrm{Var}[\xi_0(t)] = \mathrm{Var}[\eta_0(t)] = d/2$ and $\tilde{h}_{nq} = \pm 1$.

Let the waveform transmitted in the previous frame be $\tilde{s}_p(t)$, such that $h_{nm} = \tilde{h}_{nq}\tilde{h}_{np}$. Then, after the multiplier and the lowpass filter which removes the terms centered at $2\omega_n$, sampling at $t = nt_1$ yields

$$X_n = E_c([\alpha_n \tilde{h}_{np} + G_n][\alpha_n \tilde{h}_{nq} + G_{n-N}] + H_n H_{n-N}), \quad (24)$$

where $G_n$, $G_{n-N}$, $H_n$, and $H_{n-N}$ are i.i.d. Gaussian random variables with zero mean and variance $\sigma_n^2 \triangleq (\Gamma_n + d)/2$. The independence between $G_n$ and $G_{n-N}$ (same for $H_n$ and $H_{n-N}$) is approximately true because, even through the fading parameters $\beta_{kj}$ and $\theta_{kj}$ are unchanged from frame to frame, the data transmitted by the interferers are independent from frame to frame. The random variable $X_n$ is a quadratic form, extensively studied in Ref. 10, and its conditional characteristic function is given by

$$E\left[e^{iuX_n} \mid \alpha_n, \Gamma_n\right] = \left[1 + u^2 E_c^2 \sigma_n^4\right]^{-1} \exp\left[\frac{iuE_c h_{nm}\alpha_n^2}{1 - iuE_c h_{nm}\sigma_n^2}\right].$$

Averaging over $\alpha_n$, we obtain

$$E[e^{iuX_n} \mid \Gamma_n] = [1 - iuE_c h_{nm} + u^2 E_c^2 \sigma_n^2(\sigma_n^2 + 1)]^{-1}. \quad (25)$$

### 4.2 Error probability

Since the structure of the differential coherent receiver after the samplers is identical to that of the correlation receiver, the computation of error probability is the same as that in Section 3.2. The error probability for pairwise comparison is given by (12), but with

$$\Phi(z) = E_\Gamma[(1 - i2z + z^2(\Gamma + d)(\Gamma + d + 2))^{-1}]. \quad (26)$$

### 4.3 Frame synchronous case—no interference

In the interference free case ($\Gamma = 0$), $\Phi(z)$ in (26) becomes

$$\Phi(z) = (1 - i2z + z^2 d(d + 2))^{-1}$$

and has a pole at $z_0 = i/d$ in the upper half plane. Contour integration of (12) yields

$$P_p = \left(\frac{d}{2(d+1)}\right)^L \sum_{l=0}^{L-1} \binom{L-1+l}{l} \left(\frac{d+2}{2(d+1)}\right)^l, \tag{27}$$

which is identical to the expression derived by Pierce[11] for frequency-shift keying.

Figure 6 shows the performances of FHMA-DPSK and FDMA-DPSK systems for the example in Section 2.3. As in the coherent case, FHMA can accommodate the same number of users ($K = 100$) as FDMA at $P_b = 10^{-3}$, but in this case with 25 dB less power.

### 4.4 *Frame asynchronous (chip-synchronized) case*

Assuming that $\Gamma$ is binomially distributed as in Section 3.4, we perform the expectation in (26) to give

$$\Phi(z) = \sum_{k=0}^{J} B(k, J)/(1 - i2z + z^2(k+d)(k+d+2)). \tag{28}$$

which has $J + 1$ poles in the upper half plane:

$$z_k = i/(k+d).$$

Substituting (28) into (12) and using the saddle point method as in the coherent case to compute $P_p$, we plot the union upper bound of $P_b$

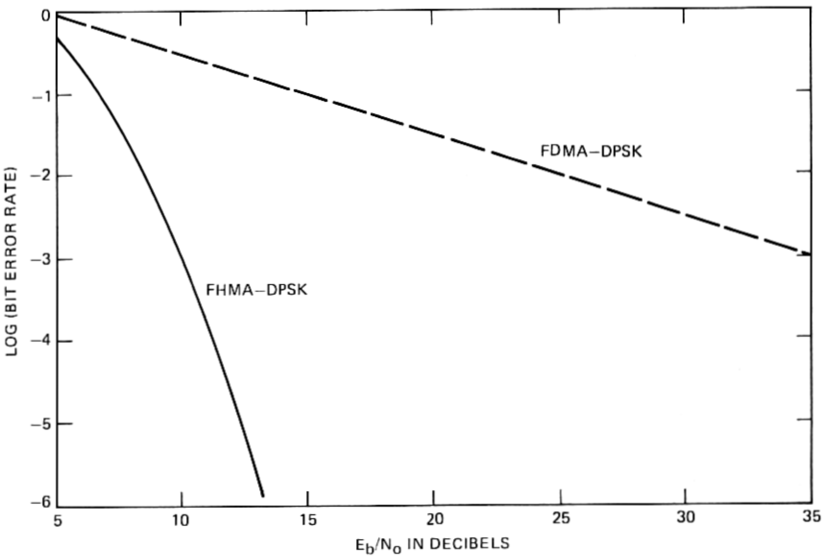


Fig. 6—Comparison between frame-synchronous FHMA and FDMA using differentially coherent PSK and Hadamard coding with rate 5/32 for 100 users sharing 100 frequency channels.

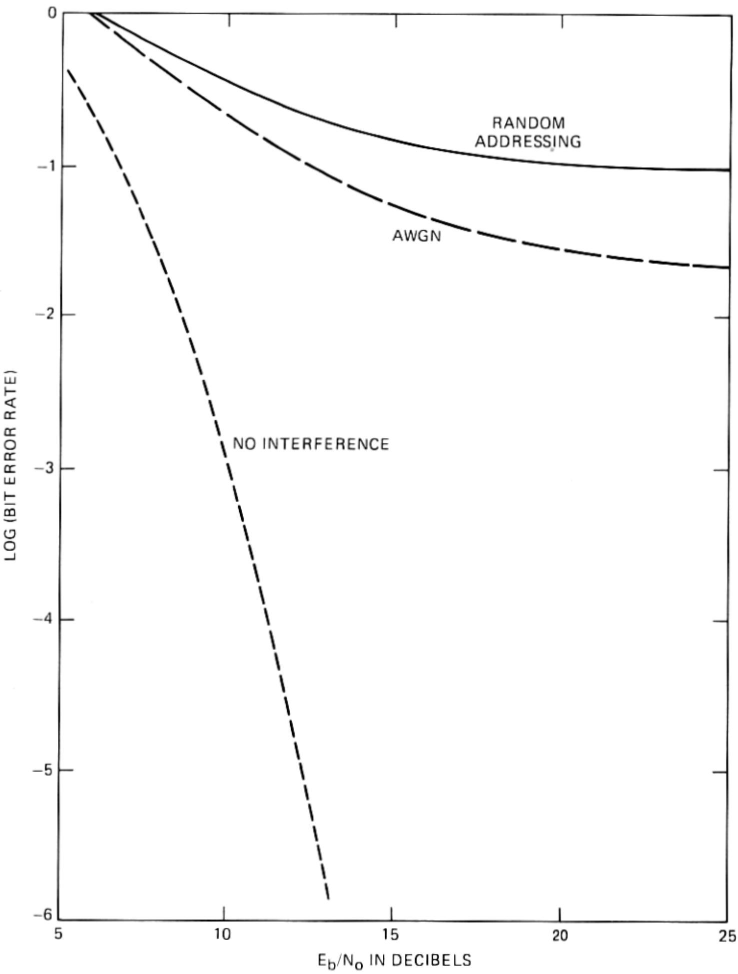


Fig. 7—Performance of frame-asynchronous FHMA-DPSK for 100 users. The AWGN result is obtained by modeling the interference as additive white Gaussian noise.

versus $E_b/N_0$ for our example with $U = J + 1 = 100$ users in Fig. 7. In contrast to the performance of the correlation receiver in Fig. 3, the upper bound in this case never goes below $10^{-3}$, which means FHMA-DPSK system cannot accommodate as many users ($U = K = 100$) as a similar FDMA-DPSK system. For the noise-free case ($d = 0$), $P_b$ is plotted as a function of the number of users in Fig. 8. We see that requiring $P_b < 10^{-3}$ would limit the number of users to about 26.

The results under the AWGN assumption are also included in Fig. 7 and 8, and they are optimistic by about 150 percent in the estimate of maximum number of users ($U = 65$) for $P_b \approx 10^{-3}$.

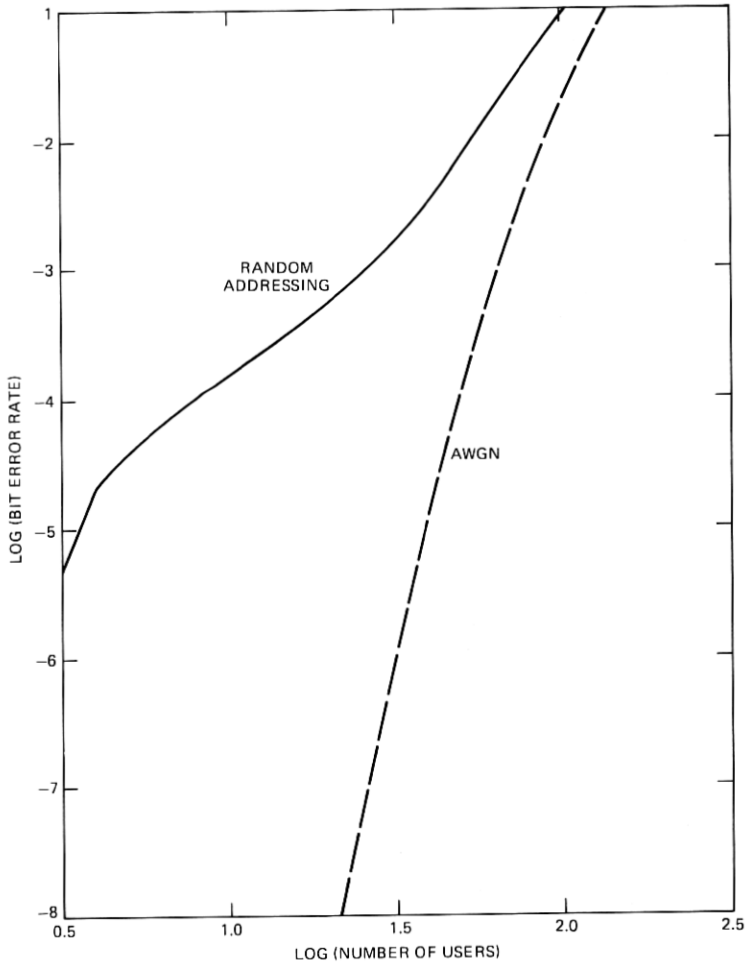


Fig. 8—Interference-limited performance of frame-asynchronous FHMA-DPSK (no receiver noise). There are 100 frequency channels available.

## V. CONCLUSIONS

In this paper, we have analyzed the performance of two FHMA-PSK systems in a Rayleigh fading environment. The primary advantage of FHMA over FDMA is the reduction of transmitted power, at the expense of equipment complexity. However, if frame synchronism cannot be maintained, the system performance is limited by user interference, and FHMA may accommodate fewer users than FDMA.

Two interference models, random addressing and AWGN, were used, and we showed that the system performance predicted by the AWGN model is too optimistic. For $f_1 t_1 < 1$ as in Ref. 1, instead of eq. (2), the probability density function of $\lambda_j$ in the frame asynchronous case would consist of a number of delta functions in $0 \leq \lambda_j \leq 1$, instead of the one [eq. (22)] and two [eq. (17)] delta functions in the AWGN and random addressing models, respectively. Then we can expect the system performance to lie between the results obtained for the two models. However, since $f_1 t_1 < 1$ causes the user addresses to be no longer orthogonal, frame synchronization among the users would not eliminate interference as in the $f_1 t_1 = 1$ case.

As an example, we considered the case of transmitting digitized speech ($R$ = 31.25 kb/s) over the mobile radio channel (bandwidth $W$ = 20 MHz) using orthogonal coding of rate $r = 5/32$, which means sending 5 bits of information with 32 bits of data. Using FDMA-PSK or FDMA-DPSK, the maximum number of users of interference-free operation is $K = r(W/R) = 100$. Without frame synchronism (but maintaining chip synchronization), the degradation of the coherent FHMA-PSK system due to user interference, for $U = K$ users, is about 5 dB in $E_b/N_0$ at $P_b = 10^{-3}$.

The frame-asynchronous performance of the differentially coherent detector for $U$ = 100 users (Fig. 7) becomes interference limited at $P_b \cong 10^{-1}$. The FHMA-DPSK system can accommodate only $U$ = 26 users if a bit error rate of $10^{-3}$ is desired. In terms of the spectral efficiency $\eta = UR/W$ b/s/Hz, FHMA-DPSK ($\eta = 0.04$) is much less efficient than FDMA-DPSK ($\eta = 0.16$) in this example. Using the AWGN interference model, we would obtain $\eta = 0.10$, which is slightly larger than Henry's result[13] because $X_n$, the quadratic form, was approximated by a Gaussian random variable in Ref. 13 (see also Ref. 12). These spectral efficiencies are applicable only to an isolated cell system; intercell interference would reduce the number of users.

In our example, if coherent detection is achievable, the equivalent bandwidth per user is 200 kHz (100 users in 20 MHz). However, for a two-way radio system employing differentially coherent detection, the number of users is limited by the performance of the mobile-to-base (frame asynchronous) link to 26, which corresponds to 770 kHz per user.

## APPENDIX

In the computation of error probability for the chip synchronized case, we have to evaluate an integral (12):

$$P_p = -\frac{1}{2\pi i}\int_c \Phi^L(z)dz/z, \tag{29}$$

with $\Phi(z)$ rewritten from (18) as

$$\Phi(z) = \sum_{k=0}^{J} \phi_k(z)(z - z_k)^{-1}, \tag{30}$$

where $\phi_k(z)$ is analytic in the upper half of the $z$-plane. Define the partial sums

$$\Phi_j(z) = \sum_{k=0}^{j} \phi_k(z)(z - z_k)^{-1} \tag{31}$$

for $j = 1, 2, \cdots, J$. Replacing $\Phi(z)$ by $\Phi_j(z)$ in (29), we obtain a monotonically increasing sequence

$$P_p(1) < P_p(2) < \cdots < P_p(J-1) < P_p.$$

The monotonicity can be seen from the fact that truncating $\Phi(z)$ to $\Phi_j(z)$ means ignoring the probabilities of more than $j$ interferers in any one chip interval.

It can be shown that there is a unique imaginary axis saddle point, $z_{sj}$, lying between the origin and $z_j$ for every $\Phi_j(z)$. Using $z_{sj}$ and $\Phi_j(z)$ in (21), we can obtain a saddle-point approximation of $P_p(j) \sim \tilde{P}_p(j)$. It was discovered in computation that $\{\tilde{P}_p(j)\}$ is not an increasing sequence in $j$ but has a maximum around $j = 10$. Without investigating the accuracy of the saddle-point approximation as a function of $j$, we surmise that, for large $j$, the saddle point is too close to the pole at $z_j$, so that $L$ has to be very large for the approximation to be accurate. Therefore in generating the curves in Figs. 3 and 4, we used the maximum of the sequence $\{\tilde{P}_p(j)\}$ as an approximation to $P_p$.

## REFERENCES


1. G. R. Cooper and R. W. Nettleton, "A Spread-Spectrum Technique for High-Capacity Mobile Communications," IEEE Trans. Veh. Tech., *VT-27* (November 1978), pp. 264–275.
2. D. J. Goodman, P. S. Henry, and V. K. Prabhu, "Frequency-Hopped Multilevel FSK for Mobile Radio," B.S.T.J., *59*, No. 7 (September 1980).
3. A. J. Viterbi, *Principles of Coherent Communication*, New York: McGraw-Hill, 1966.
4. D. C. Cox, "910 MHz Urban Mobile Radio Propagation: Multipath Characteristics in New York City," IEEE Trans. Commun., *COM-21* (November 1973), pp. 1188–1194.
5. A. J. Viterbi and I. M. Jacobs, "Advances in Coding and Modulation for Noncoherent Channels Affected by Fading, Partial Band, and Multiple-Access Interference," in *Advances in Communication Systems*, Vol. 4, A. J. Viterbi, ed., New York: Academic, 1975.
6. J. F. Pieper, J. G. Proakis, R. R. Reed, and J. K. Wolf, "Design of Efficient Coding and Modulation for a Rayleigh Fading Channel," IEEE Trans. Inform. Theory, *IT-24* (July 1978), pp. 457–468.
7. J. G. Proakis and I. Rahman, "Performance of Concatenated Dual-k Codes in a Rayleigh Fading Channel With a Bandwidth Constraint," IEEE Trans. Commun., *COM-27* (May 1979), pp. 801–806.
8. P. Bello and B. D. Nelin, "Predetection Diversity Combining With Selectively Fading Channels," IRE Trans. Commun. Sys., *CS-10* (March 1962), pp. 32–42.
9. O. Yue, "Saddle Point Approximation for the Error Probability in PAM Systems

with Intersymbol Interference," IEEE Trans. Commun., *COM-27* (October 1979), pp. 1604–1609.
10. J. E. Mazo and J. Salz, "Probability of Error for Quadratic Detectors," B.S.T.J., *44*, No. 9 (November 1965), pp. 2165–2186.
11. J. N. Pierce, "Theoretical Diversity Improvement in Frequency Shift Keying," Proc. IRE, *46* (May 1958), pp. 903–910.
12. O. Yue, "Useful Bounds on the Performance of a Spread-Spectrum Mobile Communication System in Various Fading Environments," presented at the International Conf. on Commun., June 1980.
13. P. S. Henry, "Spectrum Efficiency of a Frequency-Hopped-DPSK Spread-Spectrum Mobile Radio System," IEEE Trans. Veh. Tech. (November 1979), pp. 327–332.
14. R. W. Lucky, J. Salz, and E. J. Weldon, Jr., *Principles of Data Communication*, New York: McGraw-Hill, 1968.